GABARITO

EXAMES DE FEVEREIRO DE 2023

LÍNGUA INGLESA

TECNOLÓGICAS

Esta é a compilação do gabarito do exame PROFLIN de língua inglesa aplicado em FEVEREIRO/2023. Neste documento, você terá acesso a:

- Explicação de como acessar as questões da tentativa do(a) participante do exame, na plataforma Moodle
- Texto-base disponibilizado na plataforma Moodle, para resolução das questões;
- Questões da forma como disponibilizadas na plataforma Moodle;
- Gabarito indicando as respostas corretas para as questões de múltipla escolha, seguidas de justificativas tanto para a alternativa correta como para os distratores; respostas esperadas para as questões discursivas.

ATENÇÃO! ESTE NÃO É UM ESPELHO DO SEU EXAME PROFLIN! ESTE É UM GABARITO COM AS RESPOSTAS ESPERADAS DE TODOS OS CANDIDATOS E PODERÁ EMBASAR RECURSOS, DE ACORDO COM O QUE CONSTA EM EDITAL.

Após salvar todas as respostas da Prova, clique em "**Enviar tudo e terminar**":

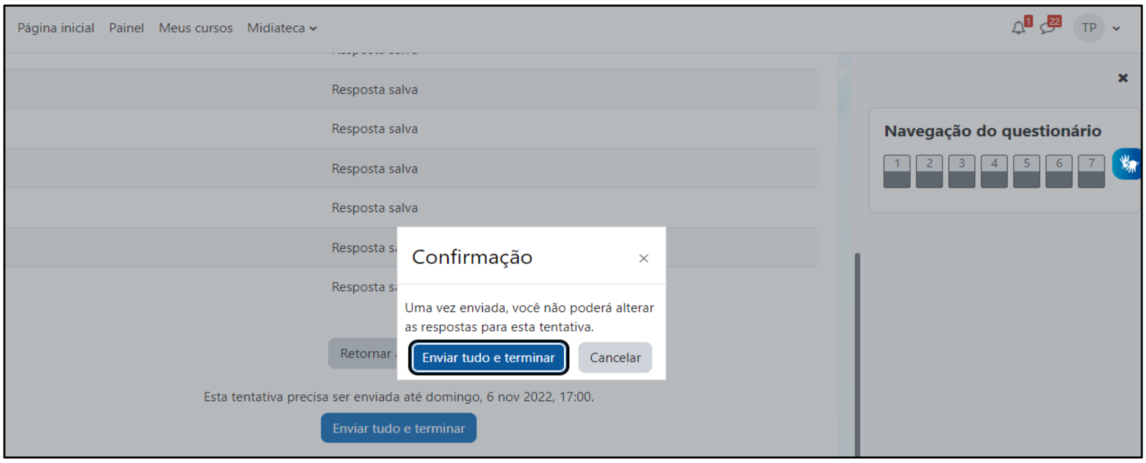

Após confirmar "**Enviar tudo e terminar**", será aberta uma página de revisão com todas as respostas que foram salvas.

Você poderá salvar ou imprimir essa página com todas as respostas que você preencheu e finalizar clicando em "**Terminar revisão**". Caso queira novamente ter acesso à página de revisão, mesmo após o término da prova, basta clicar no link "**Revisão**" estará localizado abaixo de **Resumo das suas tentativas anteriores** dentro do questionário com as Questões 1-7.

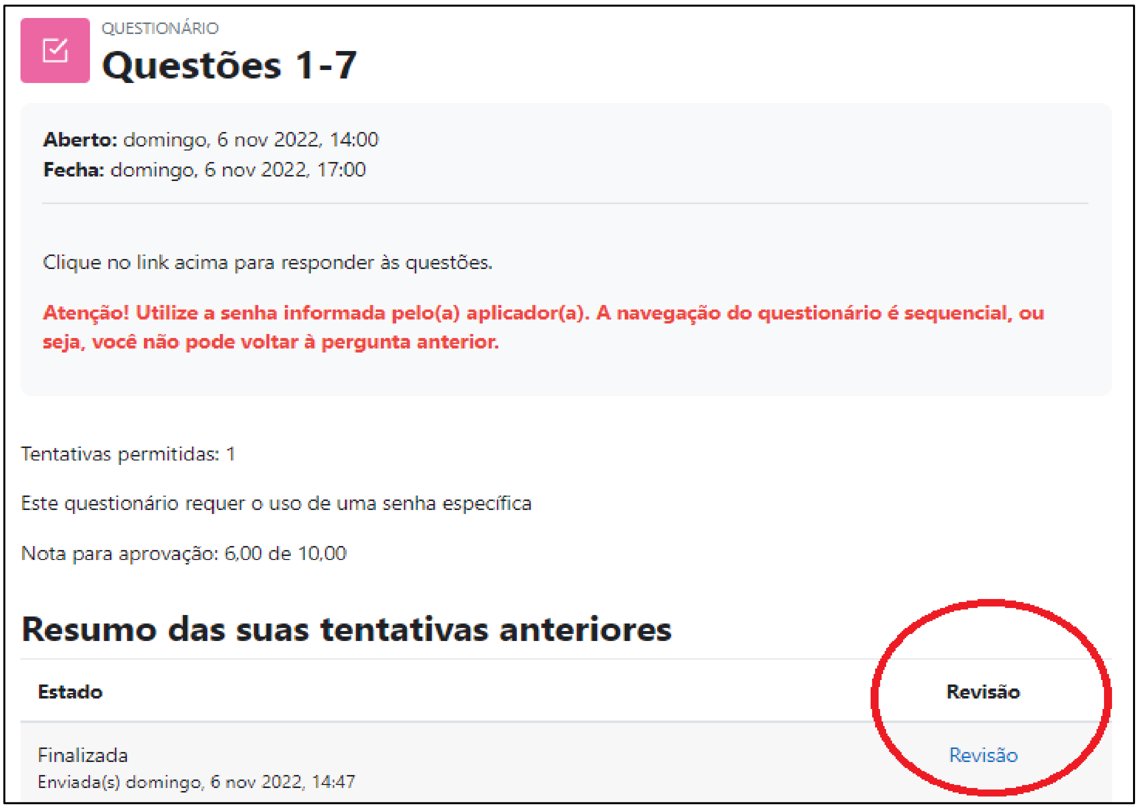

ADVANCED ENGINEERING MATERIALS
www.aem-journal.com

Multi-Material, Multi-Process, Planar, and Nonplanar Additive Manufacturing of Piezoelectric Devices

Mohammad Rafiee, Floriane Granier, Rui Tao, Abraham Bhérer-Constant, Gabriel Chenier, and Daniel Therriault**

Nonplanar multi-material additive manufacturing (AM) of piezoelectric devices is an important step for innovation in digital manufacturing. Herein this work, the development of a manufacturing platform based on multi-material multi-process AM that enables fabrication of piezoelectric and conductive electrode materials with complex planar and nonplanar (conformal) structures is reported. Also, the development of conductive and piezoelectric paste-like printing materials, herein called inks, for extrusion-based direct-writing AM processes is presented. The developed inks are highly stretchable (e.g., up to 100% before breaking), easy to process, and less toxic compared to existing solvent evaporation-based inks in the literature. Several piezoelectric energy-harvesting (PEH) devices are fabricated. The innovative inks within a multi-material multi-process 3D printing platform can substantially broaden the design space of multi-material AM and open up new opportunities for the production of application-oriented parts that are more integrable, conformable, scalable, and versatile.

1. Introduction

The multi-material extrusion-based additive manufacturing (AM) can enhance the performance of manufactured parts by adding more shape complexity and functionality.[1] Although traditional extrusion-based multi-material AM is extensively customizable, it is often limited in functionality of the printed parts due to limitation in using only one type of AM process such as fused filament fabrication (FFF) or direct ink writing (DIW) within a single machine.[2,3] Another limitation consists of only a planar approach in building the desired models by slicing a 3D model into a large set of parallel planar layers. Envisioning an evolution for AM, the ensuing step involves developing nonplanar layer-based processes and improvement of the functionality of additively manufactured components via more integrated multi-process AM that combines two or more AM processes. By using motion in all three *x*, *y*, and *z* spatial dimensions during the deposition of each layer, regardless of layer height, nonplanar layers better represent freeform surfaces than planar layers. The ability to create end-use products that contain complete circuits, sensors, optics, and other components and freeform surfaces without sacrificing the geometric benefits of AM parts is a transformative approach in digital manufacturing.[1,3,4]

Piezoelectric materials convert mechanical into electrical energy and vice versa, and have a variety of applications from actuation and pressure sensing to piezoelectric energy harvesting (PEH).[5–7] In recent years, the AM of some components of piezoelectric devices has been demonstrated.[8–13] Being self-powered further renders piezoelectric materials promising for remote location devices, human body organs, and inaccessible or confined spaces.[14,15] Although, AM of such devices is realized successfully using variety of techniques, some concerns regarding the availability and performance of materials being used for both the piezoelectric and the conductive electrode components.[14] These works are also generally limited to very simple geometries and/or suffer from multistep manufacturing that involves the fabrication of piezoelectric layer and the conductive electrodes using different manufacturing platforms.[15]

So far, a few research works have been conducted to design stretchable piezoelectric and stretchable conductive inks with characteristics such as low manufacturing cost, environmentally sustainable production method, recyclability, lightweight, low energy consumption, and ease of integration in multi-material structures.[16,17] While conductive inks received the most attention,[17–21] there is little research on the development of stretchable piezoelectric inks.[17,22,23] The inks developed in the literature are often designed for fabrication methods other than 3D printing (e.g., screen printing) and require extra heat-curing step[8,18,24] and/or high content of toxic solvents.[9,18] Additionally, complex steps involving multi-process approaches are needed to fabricate a device, which limit the scalability and facile manufacturing.

Herein, we report the design of new conductive and piezoelectric inks compatible with a manufacturing platform based on multi-material multi-process AM for the creation of complex planar and nonplanar piezoelectric and conductive structures (**Figure 1**). Specifically, we combined DIW with FFF within a single manufacturing platform to fabricate flexible and stretchable PEH devices (Figure S1, Supporting Information). In this AM platform, two printheads are equipped with a dispensing

M. Rafiee, F. Granier, R. Tao, A. Bhérer-Constant, G. Chenier, D. Therriault
Department of Mechanical Engineering
Polytechnique Montreal
Montreal, QC H3T 1J4, Canada
E-mail: mrafi005@uottawa.ca; daniel.therriault@polymtl.ca

The ORCID identification number(s) for the author(s) of this article can be found under https://doi.org/10.1002/adem.202200294.

DOI: 10.1002/adem.202200294

apparatus for DIW and one printhead is mounted with an FFF thermoplastic filament liquefier. We 3D printed several piezoelectric demonstrators and studied their piezoelectric properties and energy-harvesting performance. The experimental results showed that the fabricated piezoelectric devices possess significant piezoelectric properties for sensing and energy harvesting applications. Such materials and manufacturing development could be further employed as a fascinating tool that enables the production of various innovative material systems.

2. Results

2.1. Planar and Nonplanar AM Setup and Ink Formulation

To fabricate PEH devices, we first designed piezoelectric and highly conductive electrode inks using a thermoplastic polyurethane (TPU) matrix that embody the required rheological properties for DIW 3D printing process. Unlike prior ink designs that require extra heat-curing step,[8,18,24] and/or high content of toxic solvents,[9,18] our piezoelectric and conductive electrode inks are less toxic (with respect to existing inks in the literature[9,18]) and do not require heat cure after printing while exhibiting adequate viscosity (not too low to affect the formation of deposited filaments and not too high to make it impossible to push the material through the nozzle) desired for DIW. Specifically, we formulated the inks using TPU as the matrix, silver flakes, and barium titanate ($BaTiO_3$ also namely called BTO) as the conductive and piezoelectric fillers, and dimethylformamide (DMF) and acetone as the cosolvent system. We used BTO for their large electro-mechanical coupling coefficient, excellent dipole moment, and large dielectric constant in TPU matrix to achieve high piezoelectric properties. Being environmentally friendly and easy handling as a lead-free material also made BTO our preferred material.[25]

In DIW, the inks should be able to be extruded smoothly through dispensing nozzles (cone or cylindrical) and be able to be rapidly support itself soon after deposition, to keep the deposited material shape (**Figure 2**a). Shear rate of printing rheology shows the ink extruding capability from the nozzle. To limit evaporation of solvent, we use a solvent trap during the measurement. As shown in Figure S2, Supporting Information, a shear-thinning behavior can be observed in both Ag-TPU and BTO-TPU inks. The apparent printing shear rate is a process parameters dependent and can be approximately calculated by $4\,V/(\pi r)$, where r is the nozzle radius, and V is the printing speed.[26] In our work (nozzle diameter of 250 μm and printing speed of $10\,\mathrm{mm\,s^{-1}}$), the estimated printing shear rate is $50\,\mathrm{s^{-1}}$.

2.1.1. Ink Conductivity

The experimental data for the resistivity and conductivity of the Ag-TPU films at 0% strain as a function of silver flakes volume fractions is shown in Figure 2b with black and red triangle symbols, respectively. The conductivity of the silver film was theoretical predicted using 3D percolation theory and a power–law relationship described by $\sigma = \sigma_0\,(V_f - V_c)^s$. In this prediction, σ and σ_0 are the electrical conductivity of the silver film and the conductivity of the silver flakes, respectively. V_f and V_c are the volume fraction of the dried silver flakes, and the volume fraction (in dried form) at the percolation threshold. In the relationship, s is the power law fitting exponent. The calculated percolation threshold and the power law fitting exponent ($V_c \approx 0.08$ and $s \approx 0.911$) indicated good agreement with our experimental results. Because of their anisotropic behavior, alignment of silver flakes (**Figure 3**b) due to shear forces within the Ag-TPU ink is expected during deposition. Based on the obtained data, Ag-TPU inks composed of 55 vol% Ag was chosen

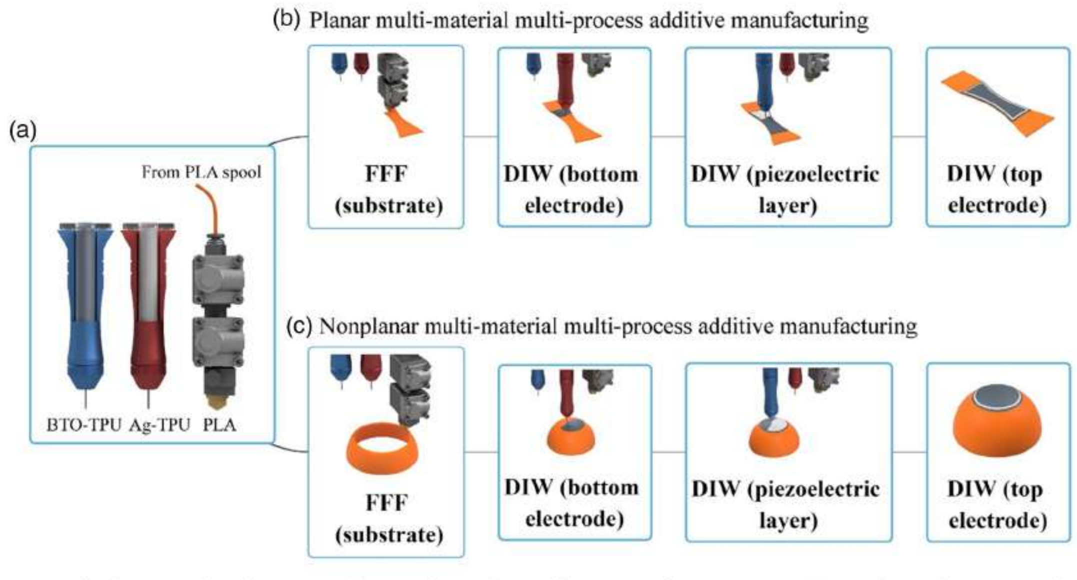

Figure 1. Schematic of multi-material multi-process planar and nonplanar additive manufacturing (AM) of piezoelectric devices: a) schematic of direct ink writing (DIW) and fused filament fabrication (FFF) printing heads containing Ag thermoplastic polyurethane (Ag-TPU), $BaTiO_3$ TPU (BTO-TPU) inks and polylactic acid (PLA) filament, b) schematic of planar AM of a multilayer piezoelectric device with varying cross section, and c) schematic of nonplanar AM of a semispherical shell (SSS) piezoelectric demonstrator.

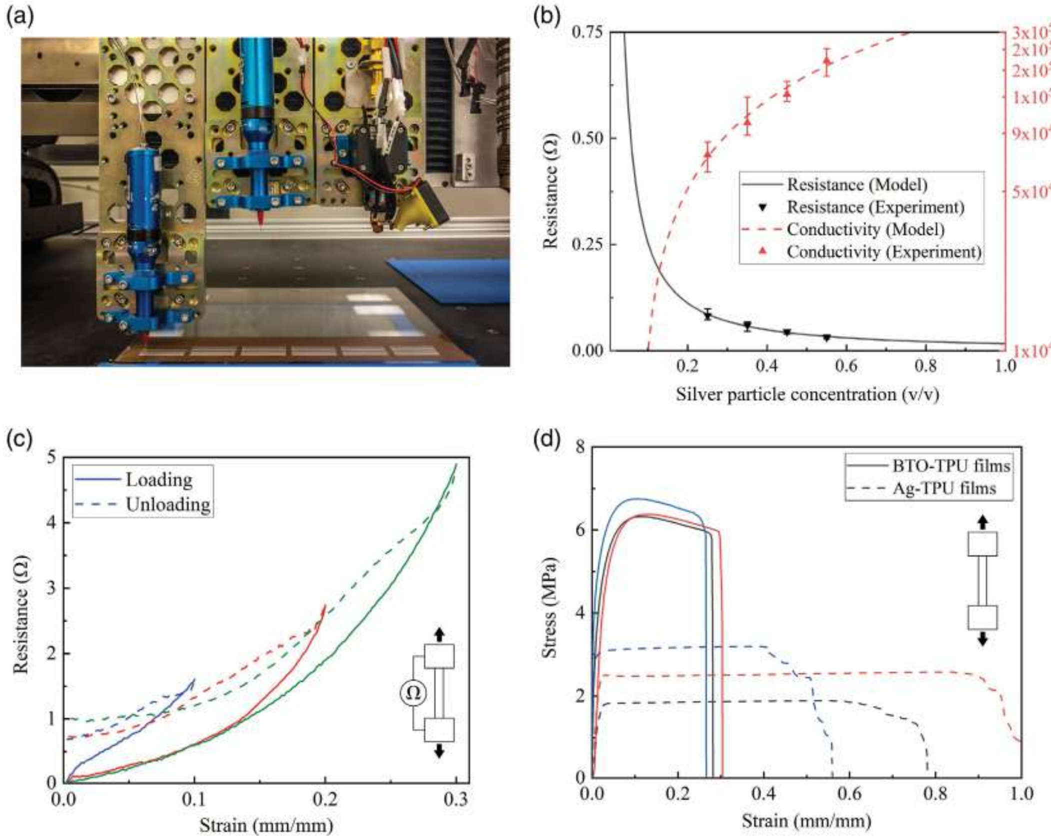

Figure 2. Characterization of inks and fabricated films: a) image of multi-material multi-process printing heads including two DIW and one FFF heads; the left DIW printing head is printing Ag-TPU ink through a 250 µm stainless steel nozzle (printed films have dimensions of 40 by 10 mm); b) electrical conductivity and resistivity of dried Ag-TPU composite films as a function of silver flake volume content. Lines are fit (triangle symbols); c) electrical resistance of Ag-TPU during 10% (blue), 20% (red), and 30% (green) of strain; d) stress–strain curves for stretched printed conductive and piezoelectric films (three repetitions for each material).

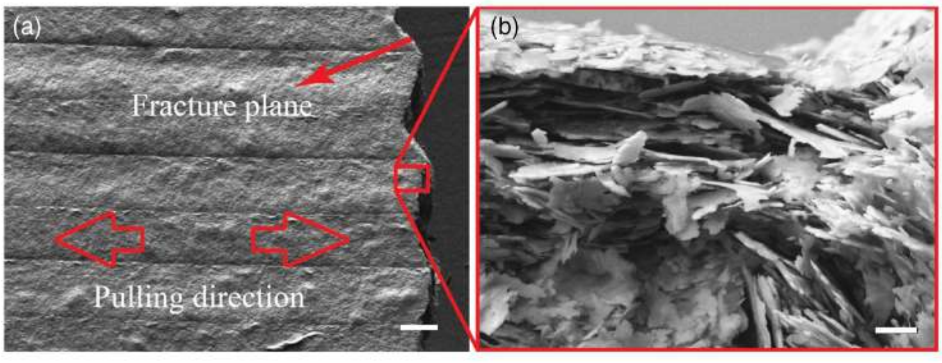

Figure 3. Scanning electron microscope (SEM) images of a single-layer Ag-TPU film after breaking a) top view (scale bar = 200 µm), b) magnified cross-sectional view (scale bar = 2 µm).

to work with, which exhibit an initial conductivity above $1.87 \times 10^5\ S\ m^{-1}$ desired for high-voltage poling and sensing applications.

It should be noted that extruding inks smoothly through dispensing nozzles is one of the limiting factors for maximum volume fraction of fillers in the TPU matrix. For instance, conductive ink with volume fraction higher than 70% by volume was not printable. Similarly, BTO-TPU ink was not printable at high content above 70% and we chose to go with 40% due to its optimum printability and adequate performance for our demonstrators.

Figure 2c shows the resistivity of the Ag-TPU films (55 vol% Ag, dimensions: $40 \times 10 \times 0.17\ mm^3$) measured under different tensile strains using four-probe electrical conductivity measurement method. The as-prepared silver films show a maximum resistivity of ≈1.61, 2.74, and 4.90 Ω at 10%, 20%, and 30% strain, respectively. The resistivities of the silver films were however reduced with unloading the strain to around 1 Ω. Mechanical hysteresis of TPUs are believed to be reason for these distinctive unloading curves.[27]

2.1.2. Stretchability of Inks

Tensile properties of both Ag-TPU and BTO-TPU films were obtained using a universal testing machine and the results are shown in Figure 2d. The tensile results indicate that the developed conductive and piezoelectric films exhibit significant stretchability properties. We printed three specimens for each of the developed inks. In Figure 2d, conductive electrode films could undergo stretchability up to ≈100% of original length while piezoelectric films could be stretched to up to 30%. This means that the conductive and piezoelectric films present enough stretchability for the fabrication of flexible or stretchable devices.

2.1.3. AM of Thermoplastic Base Layers

Thermoplastic filament made of polylactic acid (PLA) was inserted to FFF printing head to deposit the substrate material layer by layer to fabricate a 3D substrate.

Upon printing and drying of inks over the PLA substrate, piezoelectric, and conductive electrodes with track widths of approximately 250 μm that contain a percolating network of BTO nano powders or silver flakes were achieved. Figure 3a depicts a scanning electron microscopy (SEM) image of a printed silver film. Ag-TPU and BTO-TPU inks can develop a strong interface during printing. This strong interface might be due to the fact that both inks contain the same polymer matrix and solvents. Based on our vibration and bending results that will be discussed in the following section, this robust interface yields soft composite laminates that do not yield cracking or delamination during or after bending deformation. The cosolvent system being used in these ink formulations also helps to fuse the TPU ink to the PLA substrate. This adhesion is an important characteristic of these inks, since a common mode of failure in printed electronics is delamination of printed layers.[28,29]

To explain the increase in resistivity of Ag-TPU films under stretching, we carried out SEM before and after stretching at different elongations to investigate their morphologies (Figure S3, Supporting Information). From the SEM images of Figure S3, Supporting Information, a permanent distorted TPU network-silver flake and the stretch of TPU matrix (e.g., at 30% strain in Figure S3b, Supporting Information) can be seen. At a higher strain (e.g., 100% strain), electrical failure occurred in the electrodes due to disconnection of the percolative TPU network-silver flake. Considering their low resistivity, minimum variation in resistance, and high stretchability, our Ag-TPU inks are stretchable conductors with good mechanical properties.

2.2. Fabrication of PEH Devices

Our developed materials and AM platform performance was further demonstrated by 3D printing the stretchable conductive and piezoelectric inks into multilayer PEH devices with a planar or nonplanar PLA substrate as shown in **Figure 4**. Five devices namely 1) straight beam (SB), 2) variable cross-section beam (VSB), 3) S-shape beam (SSB), 4) arc-beam (AB), and 5) semispherical shell (SSS) were 3D printed.

2.3. Piezoelectric Poling

Poling is a necessary part of fabrication of piezoelectric devices. Molecular dipoles must be oriented in a single global direction within a structure. Electrical poling (Figure S4, Supporting Information) is used for this molecular dipole orientation to obtain high electromechanical transformation. As shown in Figure S4, Supporting Information, we applied an electric field of 2 kV to the sandwich structure in silicone oil medium at temperature of 80 °C. After cooling of the sample and removal of the poling electric field, most of the dipoles are locked into a configuration of near alignment known as the remnant polarization.[30]

2.4. Vibration-Based Energy Harvesting

To evaluate the PEH performance, a free and forced vibration piezoelectric testing fixture was set up to extract the voltage data from the samples. A concentrated mass of 7.5 g was added at a fixed distance from the clamped end (10 mm offset from the tip of the beams) of beam-type demonstrators shown in Figure 4b i–iv. In the free vibration testing, cantilever beam samples had one end clamped and the other end displaced to 20 mm before release. In the forced vibration test, the input signals were generated using a function generator (in sine wave format), amplified at frequency of 10 Hz and applied at the clamped end of the beams. When PEH is under vibrational load by the electrodynamic shaker, an AC electrical signal is produced. Since DC voltage is required for most electronic devices, an AC to DC full-bridge rectifier is required. Furthermore, a filtering capacitance is also required to smooth the rectified DC voltage (**Figure 5**). The voltage stored in the capacitor was measured by a digital multimeter (Fluke 87-V). The current and output were measured separately using an electrometer (Keithley 6517b). The piezoelectric voltage was collected by a charge amplifier (Piezo Lab Amplifier, MEAS Specialties). The voltage data was then transferred to a data acquisition system (NI-9239) and both current and voltage data were processed separately in a LabVIEW program.

Figure S5, Supporting Information, depicts a schematic of the forced vibration experimental setup. The setup consists of a function generator (to generate a range of vibrational frequencies) and an amplifier (to amplify the power of the signal generated by the function generator) and an electrodynamic shaker to provide a base excitation. The clamped end of all the cantilever demonstrators was attached to the electrodynamic shaker. The input signals were generated using a function generator (in sine wave format) at frequency of 10 Hz for samples shown in Figure 4bi–iv.

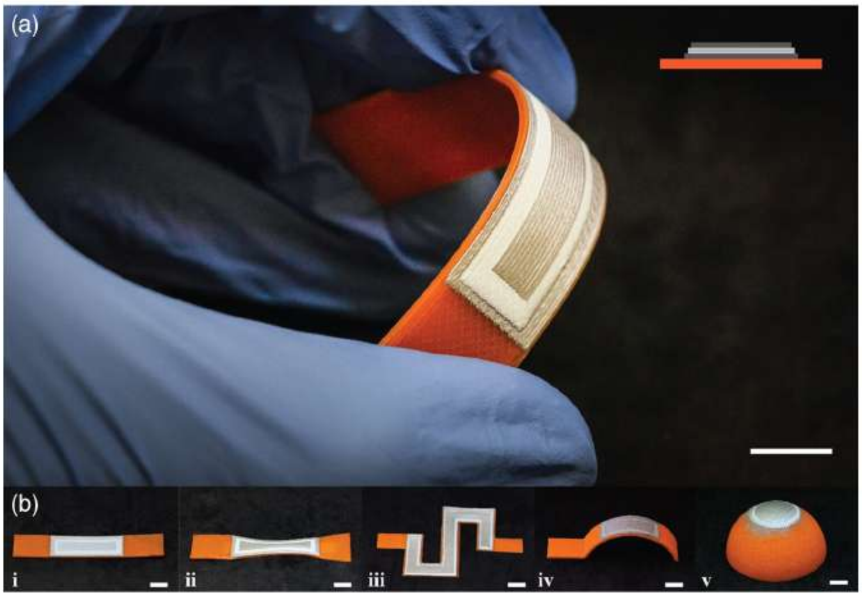

Figure 4. The 3D-printed flexible piezoelectric devices for monitoring or energy harvesting (scale bar = 10 mm): a) optical image of a flexible piezoelectric energy harvester under bending deformation; inset at the top right shows the schematic of the piezoelectric device with a PLA substrate (orange color) covered with conductive electrodes in grey color and piezoelectric layer in white color, b) piezoelectric energy-harvesting demonstrators fabricated by multi-material multi-process AM: i) straight beam (SB), ii) variable cross-section beam (VSB), iii) s-shape beam (SSB), iv) arc-beam (AB), and v) semispherical shell (SSS).

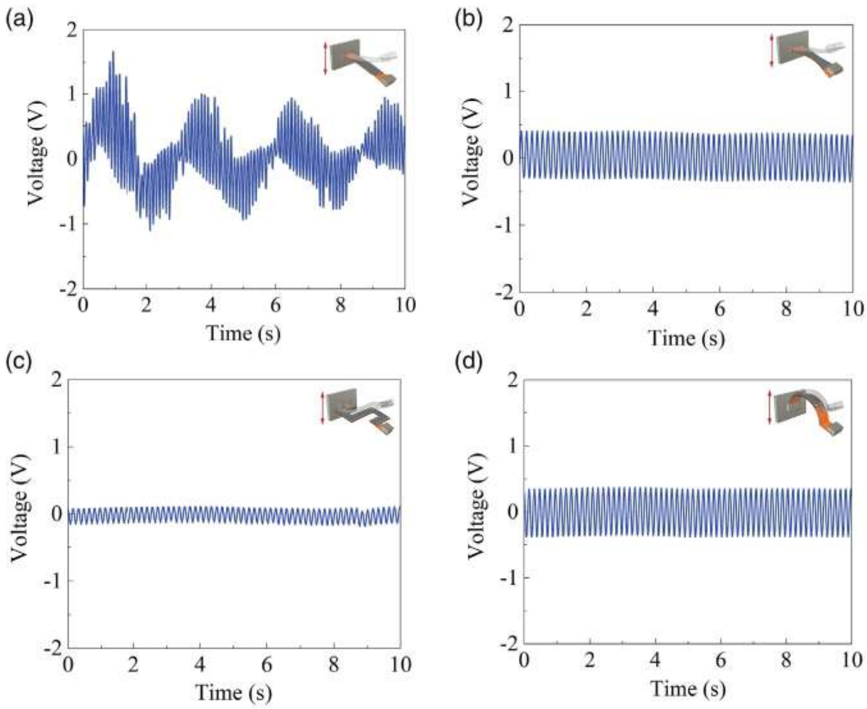

Figure 5. The open-circuit voltage measured when piezoelectric energy harvesting (PEH) devices were under forced vibration: a) SB, b) VSB, c) SSB, and d) AB. For the given input frequency and the tip mass, SB exhibits higher output voltage due to its resonance frequency closer to the excitation frequency.

The open-circuit method is widely used for PEH.[31] This conventional interface circuit includes a simple AC-to-DC power converter. We measured both AC voltage and current AC outputs as well as DC voltage being stored in the capacitor. These results can be used to further investigate the effectiveness of the developed PEH devices and their output power. The AC voltage and current responses of demonstrators under forced vibration scheme are shown in **Figure 5** and **6**. Figure 5 shows the voltage

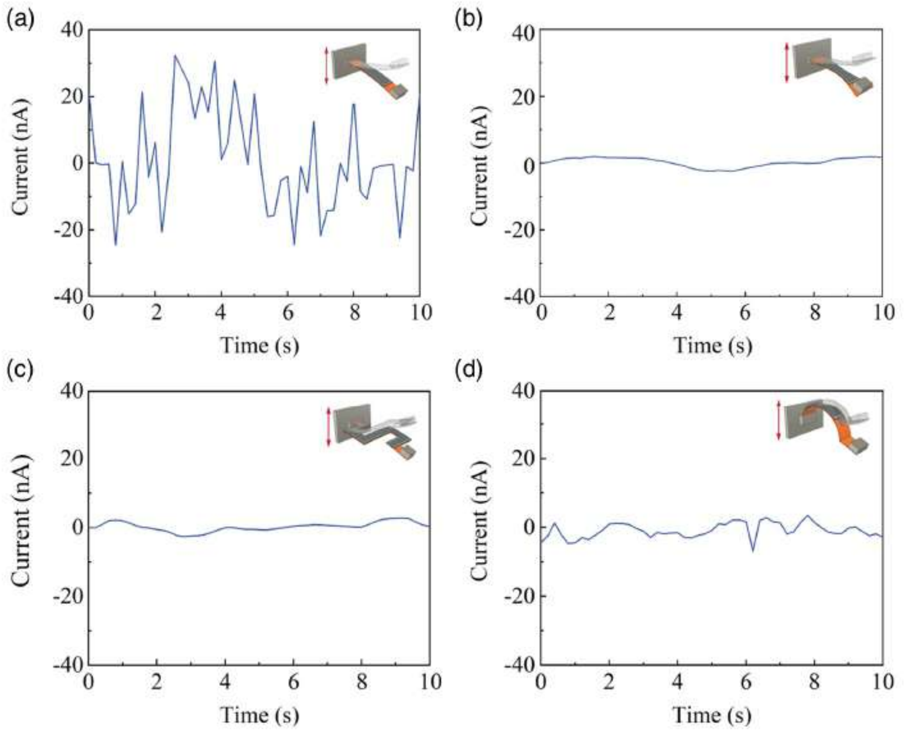

Figure 6. The open-circuit current measured when PEH devices were under forced vibration (10 × g base excitation at 10 Hz): a) SB, b) VSB, c) SSB, and d) AB. SB exhibits the highest output current due to its resonance frequency closer to the excitation frequency.

outputs measured for the four PEH devices SB, VSB, SSB, and AB with the induced open-circuit voltages of ≈2.7, 0.72, 0.25, and 0.80 V_{pp} (peak to peak voltage) at the 10 g base excitation and 10 Hz frequency, respectively. Maximum voltage or power output in a resonant system such a PEH happens when ambient vibration frequency is matched with PEH resonant frequency. If these frequencies are not matched, a significant drop in the output (voltage and power) can be obtained. Therefore, to achieve the maximum energy harvesting from each of the demonstrators, the input frequency and the tip mass must be chosen to tune the resonance frequency of their corresponding demonstrator. In this work, for the sake of simplicity, the input excitation frequency and the tip mass were considered constant values for all the forced vibration demonstrators. For the chosen input frequency and the tip mass, the demonstrators that their resonance frequency are closer to the excitation frequency exhibit higher output voltage.

A similar interpretation is valid to electrical current results. Figure 6 shows the electrical current time history for SB, VSB, SSB, and AB PEH devices. These devices were tested under the same condition with voltage results in a separate time. The scale of electric current values is in the range of sub-100 nA. This matches with our expectations and similar works in the literature.[5,32] From Figure 6, the SB produced a maximum peak current of 35 nA, which is much higher than the other three types of harvesters. Similar to the case of voltage results, the higher current values are associated with the device with excitation frequency to be near its resonance frequency. In this case, given the base excitation of 10 g and frequency of 10 Hz, SB has the resonance frequency closer to the input frequency of 10 Hz.

To verify the performance of PEHs for energy storage, we carried out experiments using the 3D-printed demonstrators in forced vibration tests to charge a capacitor (100 μF). The experimental data from the charging process of the capacitor was recorded by a digital multimeter, as shown in **Figure 7**. The capacitor voltage time history is illustrated in Figure 7, where we see the 3D-printed PEHs can charge the 100 μF capacitor to, for example, 3 mV, within 11, 27, 67, 78, and 150 s by SB, VSB, SSB, AB, and SSS, respectively.

In the free vibration test, cantilever beam specimens were fixed at one end and the other end with tip mass was manually

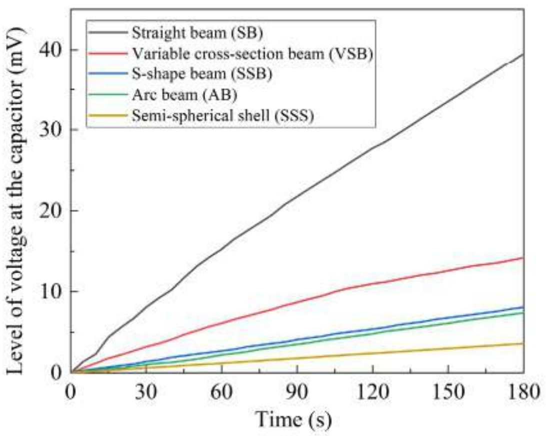

Figure 7. Capacitor voltage data for PEHs recorded during forced vibration test.

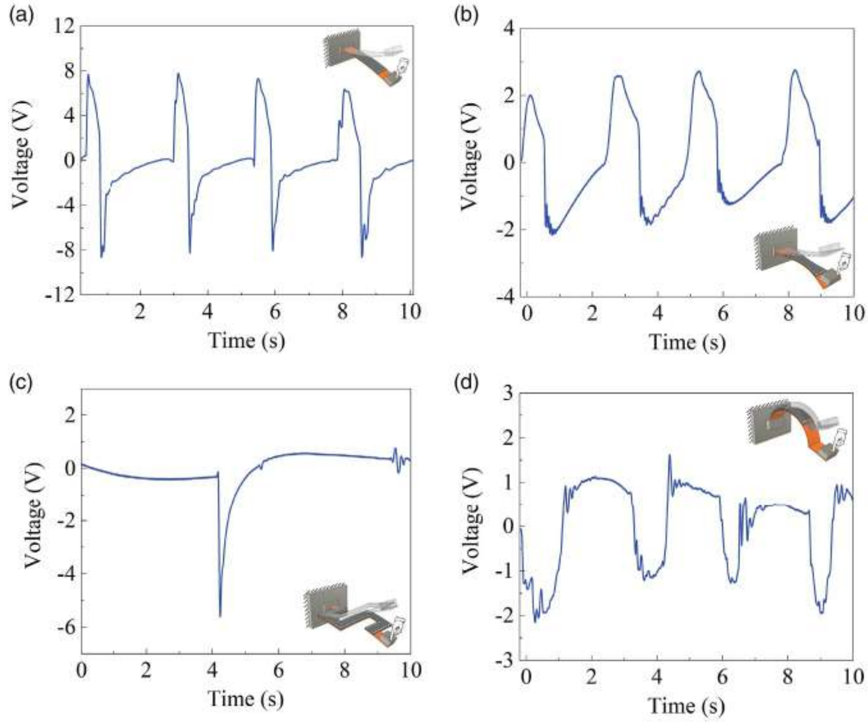

Figure 8. The open-circuit time history of voltage measured when PEH devices were under free vibration test: a) SB, b) VSB, c) SSB, and d) AB. SB exhibits the highest output current due to its resonance frequency closer to the tip excitation.

deflected to 20 mm displacement by index finger before release. The resulting voltage response was continuously recorded using the same equipment described in forced vibration test. **Figure 8** shows the first 10 s free vibration time history of the four demonstrators under the same initial displacement. Demonstrators SB, VSB, and AB were subjected to three sequences of free vibration test, and SSB, due to its spherical shape and limitation for cantilever setup, was subjected to one release of initial lateral displacement. In free vibration mode, the given initial displacement of 20 mm to the tip of cantilevers (that carry tip mass) induces a frequency that is closer to the first resonance frequency of SB demonstrator. The difference in geometry of PEHs makes the amount of stress that is being transferred from initial displacement to piezoelectric layers that vary from one configuration to another. Therefore, we expected different response from the PEHs.

Figure 9 shows the schematic as well as the output voltage and electric current for SSS PEH. The vibration and current results were measured when SSS was under lateral load. The lateral compressive load was applied by holding the demonstrator in hand and imposing $\approx$20 mm initial displacement (Figure 9a) with $\approx$2 s interval. This process was performed three times in a row. Figure 9b,c shows the measured voltage and current responses of the SSS PEH with the induced open-circuit voltage of $\approx$15 V_{pp} and the induced open-circuit maximum current of 6 nA.

In summary, we demonstrated new piezoelectric and conductive inks for multimaterial multiprocess planar and nonplanar AM of piezoelectric devices. We developed convenient, less toxic, and inexpensive formulations for fabrication of highly stretchable conductive and piezoelectric inks for DIW. The highly conductive and stretchable electrode with a high conductivity of

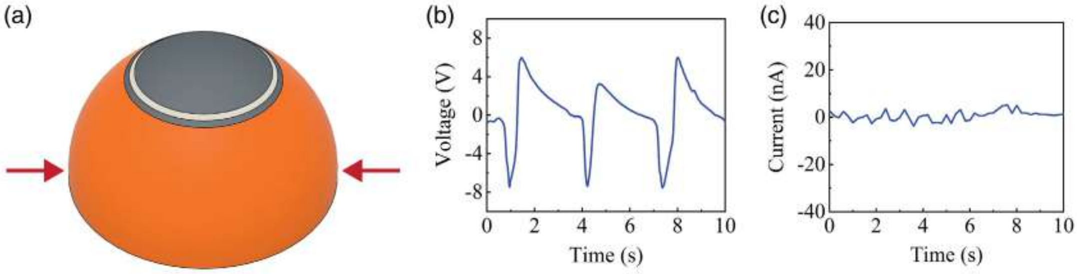

Figure 9. a) Schematic of SSS (diameter = 50 mm, wall thickness = 1 mm) under lateral compressive load; the open-circuit time history of voltage and current measured when SSS was under free vibration test: b) voltage, and c) current.

$\approx 1.87 \times 10^5$ S m^{-1} was successfully prepared using a printable silver flake–embedded TPU ink. The stretchable piezoelectric ink also showed effective performance in converting mechanical strain to electric charges. The proposed advanced technology utilized in AM of PEHs can be applied for the rapid production of energy harvesters. Importantly, the broad set of printable inks (inks made of polymer modified with either ceramics or metal particles) combined with planar and nonplanar AM offers a chance to enhance the functionality of parts made by AM (e.g., in areas such as electronics, aerospace, robotics, and textile) via this multi-material multi-process manufacturing platform.

3. Experimental Section

Materials: The stock material used as a substrate to build the PEH devices was a PLA filament (1.75 mm diameter). We dissolved TPU (85 A) in DMF (*N,N*-dimethylformamide, Sigma Aldrich) at 1:2 DMF by weight (wt/wt) to prepare TPU ink.

For production of the conductive ink, silver flakes, (Inframat Advanced Materials) with purity of 99.95% and average particle size of 2–5 μm, were added to TPU ink at 70% by weight. Acetone (Sigma-Aldrich) was then added at ratio of 1 TPU:2 acetone by weight. The mixture was ball milled for 20 min and transferred into syringes (3 cc), centrifuged at 1500 rpm for 1 h for air bubbles removal.

$BaTiO_3$ (Inframat Advanced Materials) were added to TPU ink at 40% by weight and then acetone (Sigma-Aldrich) was added at weight ratio 1 TPU:2 acetone. The mixture was ball milled for 20 min. After mixing, another dosage of acetone at weight ratio 1 TPU:2 acetone was added to lower the viscosity and the mixture was ball milled for another 20 min. The final mixture was degassed through a two-step process. In the first step, the mixture was degassed in a vacuum degassing chamber for 5 min, then transferred into 3 cc syringes, and centrifuged (to remove air bubbles) at 1500 rpm for 1 h.

Viscosity Characterization: The viscosity of all TPU, Ag-TPU, and BTO-TPU inks were measured under standard room conditions using a controlled-stress rheometer (MCR 502, Anton Paar) equipped with parallel plates (shear rates varied from 0.001 to 100 s^{-1}).

Electromechanical Characterization: Single layer Ag-TPU thin rectangular films (4 cm × 1 cm) were 3D printed. Once dried, the thickness of each sample was measured. Printed Ag-TPU films were mounted to a tensile machine (Model 50 EL, MTS Insight) and connected to a resistance measuring card (four-point method, PCI-4070 card, National Instruments) for simultaneous electromechanical characterization. Tensile tests were performed at 40 mm s^{-1}.

Planar and Nonplanar 3D Printing: The 3D printing was performed with a motion control system (ABG10000 model, Aerotech Inc., Pittsburgh, PA, USA) with four independent z-axes (see Video S1–S3, Supporting Information). Two heads were assigned for DIW (conductive and piezoelectric inks) and one head was assigned for FFF (PLA substrate). For the case of planar AM, print paths were initially generated with Simplify3D slicing software and then translated to Aerobasic language (the language of Aerotech custom-made 3D printer) using offline robotic simulation software RoboDK. In the case of nonplanar AM, the generated print paths (by Simplify3D) were projected on the surface of a cylinder or sphere using mathematical package MATLAB and then translated for gantry system using RoboDK for fabrication of AB and SSS. Extrusion of inks (via air pressure) was performed with a custom controller (MĚKANIK) using 250 μm cylindrical dispense tips (Nordson EFD) for both conductive Ag-TPU and piezoelectric BTO-TPU inks with printing speed of 10 mm s^{-1}. After printing each layer, the part was left at room temperature for evaporation of solvents (≈60 s) before printing the consequent layers. The average dried thickness of each DIW layer is 200 μm. For printing substrate, FFF process parameters such as layer thickness, feed rate, or temperature were fixed for all the devices and are shown in Table S1, Supporting Information.

Poling Process: The samples were placed inside an oil bath on a planar copper electrode connected to a high-voltage power supply (ES60, 10 W negative, Gamma High Voltage Research, Inc.) and poled under 2 kV at 80 °C for 1 h. The samples were then cooled down to room temperature before removing the electric field to avoid the misalignment of dipole moments.

Supporting Information

Supporting Information is available from the Wiley Online Library or from the author.

Acknowledgements

The financial support from National Science and Engineering Research Council (NSERC, Grant # RGPIN-2018-04566) and the Department of National Defence (DND) (Grant#: DGDND-2018-00011) are acknowledged by the authors. The first author also acknowledges Postdoctoral Scholarship from the Fonds de Recherche du Québec—Nature et Technologies (FRQNT). The authors would also like to acknowledge the technical supports from Mr. Y. Landry-Ducharme, and Drs. R. D. Farahani and K. Chizari.

Conflict of Interest

The authors declare no conflict of interest.

Author Contributions

M.R. conceptualized, designed the Ag-TPU and BTO-TPU inks and fabricated the materials and devices, poled the piezoelectric samples, characterized the piezoelectric energy-harvesting devices, contributed to the 3D schematic and illustration, and wrote the original draft. F.G. contributed to preparation Ag-TPU and BTO-TPU inks, carried out electrical conductivity/resistivity, SEM imaging and tensile characterization. R.T. contributed to poling and PEH characterization. A.B. contributed to programming of gantry system and interpretation of gcode for Aerotech gantry system. G.C. modeled the geometries and prepared the STL files, and contributed to the 3D schematics and illustrations. D.T. supervised the project, performed the project administration, and funding acquisition. All authors contributed to reviewing the writing.

Data Availability Statement

The data that support the findings of this study are available from the corresponding author upon reasonable request.

Keywords

additive manufacturing, conductive inks, direct ink writing, fused filament fabrication, multi-material 3D printing, nonplanar 3D printing, piezoelectric materials

Received: February 28, 2022
Revised: April 1, 2022
Published online: April 23, 2022

Iniciado em	sábado, 25 fev 2023, 11:26
Estado	Finalizada
Concluída em	quarta, 15 mar 2023, 09:01
Tempo empregado	17 dias 21 horas

Questão **1**

Não respondido

Vale 1,00 ponto(s).

De acordo com Rafiee *et al.* (2022), assinale a alternativa **correta**:

Escolha uma opção:

- Um material piezoelétrico autoalimentado é de uso restrito a dispositivos em lo corpo humano.
- Uma vantagem da manufatura aditiva tradicional é usar uma abordagem sor um grande conjunto de camadas planares paralelas.
- Uma limitação da manufatura aditiva tradicional é o uso de apenas um proce máquina.
- Um baixo custo de produção para o desenvolvimento de tintas piezoelétricas desenvolvidas até agora.

Questão **2**

Não respondido

Vale 1,00 ponto(s).

Qual das siglas abaixo, utilizadas no texto de Rafiee *et al.* (2002), refere-se a um dis|

Escolha uma opção:

- SSS
- FFF
- DIW
- PLA

Questão **3**

Não respondido

Vale 1,00 ponto(s).

Considerando o desenvolvimento de tinta para o experimento apresentado em Rc

Escolha uma opção:

- Os resultados indicam que os filmes condutivos e piezoelétricos desenvolvidos elasticidade.
- A interface desenvolvida entre as tintas Ag-TPU e BTO-TPU é robusta já que as diferente.
- As tintas Ag-TPU do experimento são consideradas condutores com boas prop alta rigidez.
- As tintas piezoelétricas e condutivas foram desenvolvidas utilizando um filamer (PLA).

Questão **4**

Não respondido

Vale 1,00 ponto(s).

Considerando a avaliação do desempenho dos dispositivos de coleta de energia leia as afirmativas, a seguir:

(I) Foram produzidos 5 tipos de dispositivos: i) barra reta; ii) barra com seção transve barra em formato de arco; v) concha semiesférica.

(II) A barra reta exibiu a corrente de saída mais alta devido à sua frequência de res excitação no teste de vibração forçada.

(III) No teste de vibração livre, todos os dispositivos foram submetidos a uma sequên vibrações, exceto o dispositivo em formato de concha semiesférica.

Assinale a alternativa que lista todas as afirmativas corretas de acordo com o text

Escolha uma opção:

- II, III
- I, III
- I, II, III
- I, II

Questão **5**

Não respondido

Vale 2,00 ponto(s).

Descreva a plataforma de manufatura aditiva usada para produzir os dispositivos p
apresentados no texto-base.

Questão **6**

Não respondido

Vale 2,00 ponto(s).

Rafiee *et al.* (2022) argumentam que a fórmula de tinta condutora e piezoelétrica
texto-base é mais vantajosa do que as tintas semelhantes já descritas na literatura.
apresentadas no texto, em comparação com outras tintas, de acordo com o texto

Questão **7**

Não respondido

Vale 2,00 ponto(s).

Cite e explique **duas** conclusões do artigo de Rafiee *et al.* (2022).

LÍNGUA INGLESA

TECNOLÓGICAS

TEXTO-BASE: RAFIEE, M. *et al.* Multi-material, multi-process, planar, non-planar additive manufacturing of piezoelectric devices. *Advanced Engineering Materials*. v. 24, 2022, p. 2200294 (1-9)

QUESTÃO 1:

Enunciado:

De acordo com Rafiee *et al.* (2022), assinale a alternativa **correta**:

Gabarito:

Uma limitação da manufatura aditiva tradicional é o uso de apenas um processo de manufatura aditiva em uma única máquina.

Justificativa: A alternativa está correta, conforme o seguinte trecho: “it [traditional extrusion-based multi-material AM) is often limited in functionality of the printed parts due to limitation in using only one type of AM process such as fused filament fabrication (FFF) or direct ink writing (DIW) within a single machine”.

Distratores:

1) Um material piezoelétrico auto-alimentado é de uso restrito a dispositivos em localizações remotas, como em partes do corpo humano.

Justificativa: A alternativa está incorreta. De acordo com o texto-base, um material piezoelétrico auto-alimentado é de uso promissor para dispositivos em localizações remotas e não de uso restrito, de acordo com o trecho: “Being self-powered further renders piezoelectric materials promising for remote location devices, human body organs, and inaccessible or confined spaces.”

2) Um baixo custo de produção para o desenvolvimento de tintas piezoelétricas e condutivas é tema de muitas pesquisas desenvolvidas até agora

Justificativa: A alternativa está incorreta. De acordo com o texto-base, um baixo custo de produção para o desenvolvimento de tintas piezoelétricas e condutivas é tema de poucas pesquisas e não muitas, de acordo com o trecho: "a few research works have been conducted to design stretchable piezoelectric and stretchable conductive inks with characteristics such as low manufacturing cost [...]"

3) Uma vantagem da manufatura aditiva tradicional é usar uma abordagem somente planar, fatiando um modelo 3D em um grande conjunto de camadas planares paralelas.

Justificativa: A alternativa está incorreta. De acordo com o texto-base, usar uma abordagem somente planar é uma limitação e não uma vantagem da manufatura aditiva tradicional, de acordo com o trecho: "it [traditional extrusion-based multi-material AM] is often limited in functionality of the printed parts due to limitation in using only one type of AM process […]"

QUESTÃO 2:

Enunciado:

Qual das siglas abaixo, utilizadas no texto de Rafiee *et al.* (2002), refere-se a um dispositivo não planar?

Gabarito:

SSS

Justificativa: A alternativa está correta. A sigla SSS é usada no texto-base para se referir ao dispositivo não-planar: concha semi-esférica, conforme informação na legenda da Figura 1.

Distratores:

1) FFF

Justificativa: A alternativa está incorreta. FFF significa "fused filament fabrication" e se refere a um processo de manufatura aditiva: fabricação de filamento fundido.

2) DIW

Justificativa: A alternativa está incorreta. DIW significa "direct ink writing", que se refere a um processo de manufatura aditiva: escrita direta com tinta.

3) PLA

Justificativa: A alternativa está incorreta. PLA significa "polylactic acid", que se refere ao material poliácido lático.

QUESTÃO 3:

Enunciado:

Considerando o desenvolvimento de tinta para o experimento apresentado em Rafiee *et al.* (2022), é **correto** dizer que:

Gabarito:

Os resultados indicam que o filmes condutivos e piezoelétricos desenvolvidos exibem uma propriedade significativa de elasticidade.

Justificativa: A alternativa está correta, de acordo com o trecho: "The tensile results indicate that the developed conductive and piezoelectric films exhibit significant stretchability properties."

Distratores:

1) As tintas Ag-TPU do experimento são considerados condutores com boas propriedades mecânicas, considerando sua alta rigidez.

Justificativa: A alternativa está incorreta. De acordo com o texto-base, as tintas Ag-TPU dos experimentos são condutores com alta elasticidade e não alta rigidez, de acordo com o trecho: "Considering their [...] high stretchability, our Ag-TPU inks are stretchable conductors with good mechanical properties."

2) As tintas piezoelétricas e condutivas foram desenvolvidas utilizando um filamento termoplástico feito de poliácido lático (PLA).

Justificativa: A alternativa está incorreta. As tintas piezoelétricas e condutivas foram desenvolvidas utilizando uma matriz de poliuretano termoplástico, de acordo com o trecho: "we formulated the inks using TPU as the matrix […]"

3) A interface desenvolvida entre as tintas Ag-TPU e BTO-TPU é robusta já que as tintas contêm uma matriz polimérica diferente.

Justificativa: A alternativa está incorreta. De acordo com o texto-base, as tintas contêm uma mesma matriz polimérica e não uma matriz polimérica diferente, de acordo com o trecho: "Ag-TPU and BTO-TPU inks can develop a strong interface during printing. This strong interface might be due to the fact that both inks contain the same polymer matrix and solvents."

QUESTÃO 4:

<u>Enunciado</u>:

Considerando a avaliação do desempenho dos dispositivos de coleta de energia (*energy harvesting*) por meio de vibração, leia as afirmativas, a seguir:

(I) Foram produzidos 5 tipos de dispositivos: i) barra reta; ii) barra com seção transversal variável; iii) barra em formato de s; iv) barra em formato de arco; v) concha semiesférica.

(II) A barra reta exibiu a corrente de saída mais alta devido à sua frequência de ressonância mais próxima da frequência de excitação no teste de vibração forçada.

(III) No teste de vibração livre, todos os dispositivos foram submetidos a uma sequência de três procedimentos para gerar as vibrações, exceto o dispositivo em formato de concha semiesférica.

Assinale a alternativa que lista todas as afirmativas corretas de acordo com o texto (RAFIEE, 2022):

a) I, II
b) I, III
c) II, III
d) I, II, III

<u>Gabarito</u>:

I, II

Justificativa: A alternativa está correta. A afirmação (I) está correta, de acordo com o trecho "Five devices namely 1) straight beam (SB), 2) variable cross-section beam (VSB), 3) S-shape beam (SSB), 4) arc-beam (AB), and 5) semispherical shell (SSS) were 3D printed." A afirmação (II) está correta, de acordo com o trecho: "SB exhibits the highest output current due to its resonance frequency closer to the excitation frequency"

Distratores:

1) II, III

Justificativa: A alternativa está incorreta. A afirmação (II) está correta, de acordo com o trecho: "SB exhibits the highest output current due to its resonance frequency closer to the excitation frequency." No entanto, a afirmação (III) está incorreta, de acordo com o trecho: "[…] and SSB, due to its spherical shape and limitation for cantilever setup, was subjected to one release of initial lateral displacement."

2) I, III

Justificativa: A alternativa está incorreta. A afirmação (I) está correta, de acordo com o trecho "Five devices namely 1) straight beam (SB), 2) variable cross-section beam (VSB), 3) S-shape beam (SSB), 4) arc-beam (AB), and 5) semispherical shell (SSS) were 3D printed." Porém, a afirmação (III) está incorreta, de acordo com o trecho: "[…] and SSB, due to its spherical shape and limitation for cantilever setup, was subjected to one release of initial lateral displacement."

3) I, II, III

Justificativa: A alternativa está incorreta. A afirmação (I) está correta, de acordo com o trecho "Five devices namely 1) straight beam (SB), 2) variable cross-section beam (VSB), 3) S-shape beam (SSB), 4) arc-beam (AB), and 5) semispherical shell (SSS) were 3D printed." A afirmação (II) está correta, de acordo com o trecho: "SB exhibits the highest output current due to its resonance frequency closer to the excitation frequency". Porém, a afirmação (III) está incorreta, de acordo com o trecho: "[…] and SSB, due to its spherical shape and limitation for cantilever setup, was subjected to one release of initial lateral displacement."

QUESTÃO 5:

Enunciado:

Descreva a plataforma de manufatura aditiva usada para produzir os dispositivos piezoelétricos multimateriais para os testes apresentados no texto-base.

Resposta esperada:

Espera-se que o candidato descreva a plataforma de manufatura aditiva usada para produzir os dispositivos piezoelétricos do experimento apresentado no texto-base. A resposta encontra-se no último parágrafo da seção de introdução do artigo e também pode ser observada na Figura 1. O candidato deve descrever uma plataforma de manufatura aditiva com três cabeças de impressão: duas cabeças utilizadas para dispersão por escrita direta com tinta (DIW) e uma para fabricação com filamento fundido contendo filamento termoplástico.

QUESTÃO 6:

Enunciado:

Rafiee *et al.* (2022) argumentam que a fórmula de tinta condutora e piezoelétrica desenvolvida no experimento descrito no texto-base é mais vantajosa do que as tintas semelhantes já descritas na literatura. Apresente as **três** características apresentadas no texto, em comparação com outras tintas, de acordo com o texto.

Resposta esperada:

Espera-se que o candidato apresente as três características apresentadas pelos autores. A resposta encontra-se no primeiro parágrafo da seção de resultados. De acordo com o texto-base, o primeiro passo do experimento foi desenvolver uma tinta condutiva e piezoelétrica. A tinta desenvolvida é considerada menos tóxica em comparação com as outras tintas já existentes na literatura. A tinta também não precisa de cura térmica depois da impressão. Além disso, a tinta exibe viscosidade adequada para o processo de escrita direta com tinta (DIW), que é definida no texto como uma viscosidade não muito baixa a ponto de afetar a formação dos filamentos depositados e também não tão alta a ponto de tornar impossível a passagem do material pelo bocal.

QUESTÃO 7:

Enunciado:

a) Cite e explique **duas** conclusões do artigo de Rafiee *et al.* (2022).

Resposta esperada:

Espera-se que o candidato explique, pelo menos, duas das conclusões encontradas no texto-base. A resposta encontra-se no último parágrafo da seção 2. São conclusões do texto: a) foram desenvolvidas novas tintas piezoelétricas e condutivas para uso em dispositivos piezoelétricos produzidos por manufatura aditiva multimaterial planar e não-planar; b) foram desenvolvidas fórmulas menos tóxicas e baratas para a fabricação de tinta piezoelétrica e condutiva e altamente elástica para a escrita direta com tinta (DIW); c) um eletrodo altamente elástico e condutivo foi preparado com sucesso utilizando a impressão de flocos de prata em poliuretano termoplástico (TPU); d) a tinta piezoelétrica elástica desenvolvida apresentou performance efetiva na conversão de pressão mecânica em carga elétrica; d) a tecnologia proposta para o desenvolvimento de manufatura aditiva para a coleta de energia piezoelétrica pode ser utilizada rapidamente para o desenvolvimento de coletores de energia; e) o conjunto amplo de tintas combinado com manufatura aditiva planar e não planar oferece uma oportunidade para melhorar as funcionalidades das partes produzidas por meio de manufatura aditiva por meio de uma plataforma de manufatura aditiva multimaterial e multiprocesso.